Published in final edited form as:

Retina. 2023 August 01; 43(8): 1377–1385. doi:10.1097/IAE.0000000000003815.

The Chrysanthemum Phenotype of Idiopathic Multifocal Choroiditis

Prithvi Ramtohul, MD[1], **Maria Vittoria Cicinelli, MD**[2,3], **Rosa Dolz-Marco, MD, PhD**[4], **Orly Gal-Or, MD**[5,6], **Sarah Mrejen, MD**[7], **Jesús R García-Martínez, MD**[8], **Alla Goldberg, MD**[9], **Eduardo Cunha de Souza, MD**[10], **Elisabetta Miserocchi, MD**[2,3], **Emmett T. Cunningham Jr, MD, PhD, MPH**[11,12,13], **Lawrence A. Yannuzzi, MD**[1], **K. Bailey Freund, MD**[1,14], **Edmund Tsui, MD**[15]

[1]Vitreous Retina Macula Consultants of New York, New York, New York, USA.

[2]Department of Ophthalmology, IRCCS San Raffaele Scientific Institute, Milan, Italy.

[3]School of Medicine, Vita-Salute San Raffaele University, Milan, Italy.

[4]Unit of Macula, Oftalvist Clinic, Valencia, Spain.

[5]Department of Ophthalmology, 36632 Rabin Medical Center - Beilinson Hospital, Petach Tikva, Israel.

[6]Sackler Faculty of Medicine, 58408Tel Aviv University, Tel Aviv, Israel.

[7]Ophthalmic Center for Imaging and Laser, Paris, France.

[8]Oftalvist Clinic, Madrid, Spain.

[9]Ruiz Department of Ophthalmology and Visual Science, McGovern Medical School at The University of Texas Health Science Center at Houston (UTHealth), Houston, Texas, USA.

[10]Department of Ophthalmology, University of São Paulo (USP), SP, Brazil.

[11]The Department of Ophthalmology, California Pacific Medical Center, San Francisco, CA, USA.

[12]The Department of Ophthalmology, Stanford University School of Medicine, Stanford, CA, USA.

[13]The Francis I. Proctor Foundation, UCSF School of Medicine, San Francisco, CA, USA.

[14]Department of Ophthalmology, NYU Grossman School of Medicine, New York, New York, USA

[15]Ocular Inflammatory Disease Center, UCLA Stein Eye Institute, David Geffen School of Medicine at UCLA, Los Angeles, California.

Abstract

Purpose: To describe the clinical characteristics and multimodal imaging (MMI) features of a distinctive subtype of active idiopathic multifocal choroiditis (iMFC) lesions with grey-yellow chorioretinal lesions surrounded by smaller satellite dots, a presentation referred to as “chrysanthemum lesions”.

Corresponding author: Edmund Tsui, M.D., UCLA Stein Eye Institute, 100 Stein Plaza, Los Angeles, CA 90095-7000. etsui@mednet.ucla.edu.

Methods: Retrospective, observational, multi-center case series of eyes with active iMFC and chrysanthemum lesions. Multimodal imaging features were reviewed and presented.

Results: Twenty-five eyes from 20 patients (12 women and 8 men), with a mean age of 35.8±17.0 years (range, 7 – 78 years) were included. Chrysanthemum lesions were equally located in the macula (48.0%) or the mid/far-periphery (52.0%). The number of lesions per eye varied from 1 (16.0%) to more than 20 (56.0%). On optical coherence tomography (OCT), chrysanthemum lesions showed typical features of iMFC, including subretinal hyperreflective material splitting the retinal pigment epithelium/Bruch's membrane (RPE/BrM). Chrysanthemum lesions were hypoautofluorescent on fundus autofluorescence imaging, hyperfluorescent on fluorescein angiography, hypofluorescent on indocyanine green angiography, and associated with choriocapillaris flow signal deficit on OCT-angiography.

Conclusion: Active iMFC may present with findings resembling chrysanthemum lesions. The distinctive lesion morphology on ophthalmoscopic examination, the high number of lesions, and the high prevalence of exclusive mid- and far-peripheral involvement may represent a distinctive phenotype of iMFC.

Summary statement:

In this case series of 25 eyes, we describe and analyze the clinical and multimodal imaging features of the chrysanthemum phenotype of idiopathic multifocal choroiditis.

Keywords

chrysanthemum; multifocal choroiditis; MEWDS; multimodal imaging; optical coherence tomography; punctate inner choroidopathy

Introduction

Idiopathic multifocal choroiditis (iMFC) is an inflammatory disorder of unknown etiology presenting predominantly in young, healthy, myopic women with decreased vision, scotomas, photopsia, floaters, and/or metamorphopsias.[1–3] Although the etiopathogenesis remains unclear, iMFC may represent the ocular manifestation of an autoimmune disease in genetically susceptible patients.[4] Gass further hypothesized that iMFC belongs to the acute zonal occult outer retinopathy (AZOOR) complex, a collection of syndromes that includes AZOOR and the several other white spot syndromes (i.e., multiple evanescent white dot syndrome [MEWDS] and punctate inner choroiditis [PIC]).[5] There is now evidence that iMFC and PIC may be the same disorder, with the term "PIC" traditionally used to describe eyes presenting with mild disease lacking vitritis and limited to the macular region.[6,7]

Clinically, eyes with active iMFC lesions are characterized by minimal or no anterior and/or posterior segment inflammation and multiple grey-yellow chorioretinal lesions that evolve typically into punched-out chorioretinal atrophy ranging from 50 to 350 μm in the posterior pole and periphery, sometimes clustering in curvilinear streaks or Schlaegel lines.[6,8–10] On optical coherence tomography (OCT), active iMFC lesions correspond to subretinal material of medium reflectivity splitting the retinal pigment epithelium/Bruch's membrane (RPE/BrM) complex and are associated with posterior

hypertransmission and focal choroidal thickening with loss of the normal choroidal architecture (i.e., inflammatory pigment epithelial detachment [PED]).[6,11] Prompt treatment with local or systemic corticosteroids may improve the visual acuity; nonetheless, a high risk of secondary choroidal neovascularization (CNV) and subretinal fibrosis exists, warranting long-term follow-up and appropriate management using intravitreal injection of anti-vascular endothelial growth factor (VEGF).[12]

Advances in multimodal imaging (MMI) have helped refine specific clinical characteristics of white spot syndromes, including iMFC. We have observed iMFC patients presenting with active grey-yellow chorioretinal lesions surrounded by smaller satellite dots in the macula or the mid/far-periphery. These findings resemble the appearance of a chrysanthemum and as such have been termed “chrysanthemum lesions” (personal communication, Lawrence A. Yannuzzi, MD).

This study aims to describe the clinical, MMI, and natural history features of chrysanthemum iMFC, heretofore unreported.

Methods

This is an observational, retrospective, multi-center case series of iMFC patients presenting with chrysanthemum lesions. Each coauthor identified compatible cases using patient lists, keywords, or diagnostic indicators applied to their database from 2010 to 2022. This study was approved by the Western Institutional Review Board (Olympia, WA), and written informed consent was not required due to the retrospective nature of this study. This report adhered to the tenets of the Declaration of Helsinki and complied with the Health Insurance Portability and Accountability Act.

The inclusion criteria were eyes with findings on clinical examination or MMI consistent with iMFC and showing findings consistent with chrysanthemum lesions, defined as a central grey-yellow lesion, with varying degrees of hyperpigmentation, involving the RPE and outer retina surrounded by multiple pale satellite dots. Patients were excluded if they had a known history of ocular histoplasmosis or systemic diseases known to cause MFC. A targeted medical evaluation and laboratory testing were performed for each patient and were uniformly negative for infectious or systemic diseases associated with MFC lesions (e.g., tuberculosis, syphilis, or sarcoidosis).

All patients underwent a complete ophthalmologic examination, including measurement of the best-corrected visual acuity (BCVA) using Snellen charts, slit-lamp biomicroscopy, and indirect fundus ophthalmoscopy. Color fundus photographs (EIDON AF, Centervue Padova, Italy or Topcon TRC-50IX retinal camera, Topcon Medical Systems, Oakland, NJ or Optos plc, Dunfermline, Scotland), spectral-domain OCT (OCT; Spectralis, Heidelberg Engineering, Heidelberg, Germany), swept-source OCT and OCT-angiography (OCTA, PLEX Elite 9000, Carl Zeiss Meditec, Inc, Dublin, CA), near-infrared reflectance imaging (Spectralis, Heidelberg Engineering, Heidelberg, Germany), fundus autofluorescence imaging (FAF, Spectralis HRA, Heidelberg Engineering, Heidelberg, Germany or Optos, plc, Dunfermline, Scotland), fluorescein (FA) and indocyanine green angiography (ICGA,

Spectralis HRA, Heidelberg Engineering, Heidelberg, Germany or Optos, plc, Dunfermline, Scotland) were reviewed when available. The location of chrysanthemum lesions was subdivided into posterior pole, mid-periphery, and far-periphery, according to the International Widefield Imaging Study Group.[13]

Detailed chart reviews were performed, and deidentified demographic and clinical data, including ages, genders, refraction, presenting symptoms, ocular and systemic medical history, ocular and systemic therapies, and baseline and final Snellen BCVA, were collected and summarized. The Snellen BCVA were converted to logarithm of minimum angle of resolution (logMAR) for analysis. Quantitative and qualitative data are presented as mean ± standard deviation and median, and absolute and relative proportions, respectively.

Results

Demographic data

Twenty-five eyes from 20 patients (12 women and 8 men) were included. The mean age was 35.8 ± 17.0 years (range, 7 – 78 years; median, 34.0 years) and the mean follow-up duration was 15.5 months (range, 3 – 96 months; median, 12.0 months). All but one eye were myopic (96.0%) and the mean spherical equivalent was −5.50 diopters (range, −12.0 to 0 diopters; median: −3.25 diopters). Involvement was unilateral in 64.0% of eyes at diagnosis; all patients showed iMFC findings in the fellow eye during the follow-up (i.e., acute iMFC lesions or iMFC scars including punched-out chorioretinal lesions, Schlaegel lines or peripapillary atrophy). At presentation, the mean BCVA was 0.22 logMAR (Snellen equivalence, 20/33; range, 20/200 – 20/20) and improved to 0.11 logMAR (Snellen equivalence, 20/26; range, 20/70 – 20/20) at the end of the follow-up. Treatments initiated at presentation included oral corticosteroids (90.0%), periocular corticosteroids (10.0%), and long-term immunosuppressive therapy (10.0%, methotrexate or mycophenolate mofetil).

Presenting symptoms were acute vision loss in 15 patients (75.0%), scotomas in 5 patients (25.0%), and photopsia in 1 patient (5.0%). Ocular history was unremarkable in all cases, and systemic medical history included autoimmune thyroiditis in 1 patient (5.0%) and recent COVID-19 infection in 1 patient (5.0%), respectively. Table 1 summarizes the demographic and clinical data.

Ophthalmoscopic features

On ophthalmoscopic examination, chrysanthemum lesions were characterized by a grey-yellow central lesion (*the core*), some with varying degrees of hyperpigmentation, surrounded by pale satellite dots (*the petals*). Lesions were located at the posterior pole in 48.0% of eyes; in the remaining eyes (52.0%), chrysanthemum lesions involved the mid- and far-periphery exclusively. The presence of chrysanthemum lesions at the posterior pole was significantly associated with a mean BCVA < 0.3 logMAR (Snellen equivalent, 20/40; Pearson correlation coefficient $r = 0.85$; $P < 0.01$). The number of lesions per eye varied from 1 (16.0%), between 2 and 19 (28.0%), between 20 and 49 (40.0%), to more than 50 (16.0%). At presentation, chrysanthemum lesions were the only iMFC findings in 52.0% of eyes. The remaining eyes also showed peripheral punched-out chorioretinal scars

(40.0%), Schlaegel lines (4.0%), and peripapillary atrophy (4.0%). Mild anterior chamber inflammation and vitritis were noted in 16.0% of eyes.

Multimodal imaging features

On cross-sectional OCT, chrysanthemum lesions showed subretinal iso/hyperreflective material splitting the RPE/BrM complex, downwardly deflected BrM, RPE/BrM complex defects, and posterior choroidal hypertransmission. Satellite dots corresponded to small iMFC lesions causing RPE/BrM disruption and alteration of the ellipsoid zone (EZ) and interdigitation zone (IZ). The underlying choroid showed focal thickening and loss of the normal choroidal architecture. The mean subfoveal choroidal thickness was 411.5 ± 235.0 μm (range, 30 – 655 μm).

The core and satellite dots of the chrysanthemum lesions were hypoautofluorescent on FAF imaging, hyperfluorescent on early and late FA, and hypofluorescent on early and late ICGA. On OCTA, the chrysanthemum lesions co-localized with areas of choriocapillaris and inner choroidal flow signal deficits. Table 2 summarizes the MMI features of chrysanthemum lesions. Figures 1 and 2 show representative cases of peripheral and macular chrysanthemum lesions on MMI, respectively.

Evolution and complications

During the follow-up period and under corticosteroid treatment, ophthalmoscopic examination and OCT imaging showed rapid resolution of the chrysanthemum lesions with a legacy of outer retinal/RPE/BrM atrophy and varying degrees of RPE pigmentation (64.0%). The size of the outer retinal/RPE/BrM scars encompassed the whole active lesions (core and satellite dots). Thirty-two percent of the eyes developed subretinal fibrosis and 20.0% were complicated with CNV requiring intravitreal anti-VEGF therapy. The development of CNV was significantly associated with the presence of chrysanthemum lesions at the posterior pole (Pearson correlation coefficient $r = 0.92$; $P < 0.01$). In one eye, the resolution of the equatorial chrysanthemum lesions was followed by Schlaegel line enlargement and elongation. Recurrences of the chrysanthemum lesions were noted in 36.0% of eyes, with 1 (50.0%) to 2 (50.0%) recurrent events during the follow-up period. One third of these eyes (33.3%) had chrysanthemum lesions recurrence at the same location. New chrysanthemum lesions occurred at different retinal locations in the remaining eyes. Figure 2 shows the MMI of a recurrent chrysanthemum lesion.

Concurrently with the chrysanthemum lesions, an epiphenomenon MEWDS (EpiMEWDS)[14] was observed in 60.0% of patients and was associated with vision loss when involving the fovea. EpiMEWDS was characterized by EZ/IZ disruption on OCT, hyperautofluorescent spots on FAF imaging, early and late hyperfluorescence on FA, and late hypofluorescence on ICGA. Figure 3 shows the MMI of active chrysanthemum lesions complicated with EpiMEWDS. During the early course of EpiMEWDS, a hyperautofluorescent rim surrounded the chrysanthemum lesions and subsequently expanded over time. Resolution of EpiMEWDS was observed within 8 weeks in all cases and was associated with visual acuity improvement coinciding with restoration of the EZ/IZ bands on OCT, and disappearance of the hyperautofluorescent spots on FAF imaging. EpiMEWDS

and chrysanthemum lesions evolved independently; while chrysanthemum lesions showed a robust response to corticosteroid therapy, EpiMEWDS showed paradoxically initial extension with secondary resolution over weeks.[11] Figure 4 shows the differential evolution of chrysanthemum lesions and EpiMEWDS under corticosteroid therapy.

Discussion

In this study, we summarize the clinical, MMI, and natural history findings of inflammatory chorioretinal lesions resembling a chrysanthemum in patients with active iMFC. Demographic data of our patients were consistent with the epidemiology of iMFC as most of the patients were young, otherwise healthy, myopic females. All eyes developed typical iMFC scars (i.e., punched-out chorioretinal lesions, Schlaegel lines, peripapillary atrophy, and subretinal fibrosis) over the follow-up period. OCT showed characteristic splitting of the RPE/BrM complex by iso/hyperreflective material, focal choroidal thickening, and posterior hypertransmission in the acute phase. Additional MMI findings supported inflammatory involvement of the inner choroid. Therefore, all MMI features were consistent with iMFC and suggested that chrysanthemum lesions were not a separate disease but rather a specific subtype of iMFC.

Besides typical iMFC features, chrysanthemum lesions were characterized by a distinctive morphology on MMI, a high number of lesions (more than 20 lesions per eye in half of the cohort), and a high prevalence of exclusive mid- and far-peripheral involvement. As half of the eyes had no additional iMFC findings at first presentation, chrysanthemum lesions might be easily overlooked on ophthalmoscopic examination or misdiagnosed as degenerative chorioretinal lesions in highly myopic eyes. Recognition of the MMI pattern of chrysanthemum lesions may be helpful to correctly diagnose patients with iMFC.

To our knowledge, the chrysanthemum phenotype of iMFC has not been defined explicitly in the literature, but a similar pattern has been reported previously.[15–17] For instance, Cunha de Souza reported an atypical case of iMFC presenting with petaloid-shaped lesions consistent with our description of the chrysanthemum iMFC.[17] We hypothesized the distinctive shape of chrysanthemum lesions characterized by a central lesion and satellite smaller dots may be due to the subretinal eruption and centrifugal spreading of inflammatory choroidal infiltrates. In fact, focal interruption of the RPE/BrM complex by the chrysanthemum lesion was a common imaging finding on OCT. Moreover, pre-existent choroidal venous congestion or pachychoroid disease may also influence the iMFC manifestations.[18] This is supported by the increased choroidal thickness found in our study compared with the expected choroidal thickness assessed in a dataset of high myopic eyes.[19,20] Further comparative studies are required to confirm this assumption. Chrysanthemum lesions may evolve into punched-out chorioretinal atrophy and may coalesce into Schlaegel lines. Somkijrungroj et *al.* reported a case of atypical iMFC lesions resembling a chrysanthemum that developed Schlaegel lines after resolution of the active equatorial iMFC lesions.[15] Similarly, one patient from our cohort had Schlaegel line extension after regression of the active lesions, reinforcing the hypothesis that chrysanthemum lesions contribute to Schlaegel line formation in iMFC.

Given the high number of active lesions and the predilection for peripheral involvement, the chrysanthemum subtype of iMFC should be distinguished from placoid chorioretinitis, including relentless placoid chorioretinitis (RPC), which is characterized by creamy deep numerous (< 50) lesions scattered throughout the fundus and outer retinal and RPE disruption with loss of the normal choroidal architecture on OCT imaging.[21,22] Similarly, RPC lesions are typically hyperfluorescent on late-phase FA, hypofluorescent on late-phase ICGA, and show choriocapillaris flow signal deficit on OCTA.[21,22] However, the specific morphology of the lesions (chrysanthemum *versus* placoid-like lesions), the distinct clinical course (exquisite response to corticosteroid therapy for chrysanthemum iMFC *versus* continuous progression despite corticosteroid treatment for RPC), and the OCT angular sign of Henle fiber layer hyperreflectivity (ASHH) in the acute phase of RPC may be helpful to differentiate the two conditions.[23,24]

Multimodal imaging analyses helped expand the clinical spectrum of iMFC. Jung et *al.* described a series of iMFC patients presenting with an uncommon pattern of zonal or diffuse outer retinal or chorioretinal atrophy.[25] Recently, Moussa et *al.* characterized serpiginous-like peripapillary chorioretinal atrophy in a cohort of iMFC patients.[26] Chen et *al.* proposed the term “streaky MFC” to describe linear streak formation in young women with rapidly progressive myopia and iMFC.[27] Our group recently described the occurrence of iMFC lesions in patients with unrelated chorioretinal diseases and suggested that loss of the immune privilege due to pre-existent RPE/BrM complex disruption may trigger iMFC lesions in susceptible patients.[28] Moreover, several studies reported acute transient photoreceptor disruption surrounding iMFC lesions.[14,29,30] In this study, 60.0% of eyes presented with transient reversible photoreceptor alteration, called EpiMEWDS or MEWDS-like reaction.[14,29] Interestingly, EpiMEWDS first occurred in the proximity of chrysanthemum lesions and subsequently extended centrifugally.[11] The paradoxical worsening after corticosteroid therapy and the asynchronism with iMFC lesions may suggest different inflammatory pathways.[11] Nonetheless, the occurrence of two white spot syndromes (i.e., iMFC and MEWDS) in the same eye may support a common inciting retinal insult and a shared genetic predisposition.[30]

Definitive recommendations regarding therapeutic management cannot be provided owing to the limited number of cases. In our study, chrysanthemum lesions were rapidly responsive to corticosteroid therapy in all cases. Classic complications of iMFC, including CNV and inflammatory recurrences,[12] were seen in more than half of the eyes. A combination of intravitreal anti-VEGF injections and immunosuppressive therapies may be required to control longer term iMFC complications and to achieve favorable visual outcomes in a majority of patients.

Limitations of this study include the retrospective nature, the relatively small sample size, and the incomplete MMI data in some cases. Although we reviewed the medical records for causes of secondary MFC, we cannot exclude the presence of an undiagnosed condition. Moreover, the limited sample size, lack of a control group or standardized treatment or follow-up prevent any definitive conclusions regarding optimal management.

In summary, we report a series of patients presenting with MMI findings consistent with active iMFC, but with a distinctive phenotype herein called chrysanthemum lesions. Notable features included central grey-yellow chorioretinal lesions surrounded by smaller satellite dots, often numerous and involving the mid- and far-periphery in a high number of patients. Ultra-widefield imaging techniques may help to identify lesions well anterior to the macula. Despite exquisite response to corticosteroid therapy, typical complications of iMFC were frequent, including high rates of both CNV formation and inflammatory recurrences. This paper may aid in prompt recognition and treatment of this distinctive iMFC phenotype.

Funding/Support:

This work was supported by The Macula Foundation Inc., New York, New York, USA. Prithvi Ramtohul was supported by The Philippe Foundation.

Financial disclosures: K. B. Freund is a consultant for Heidelberg Engineering, Zeiss, Allergan, Bayer, Genentech, and Novartis and receives research support from Genentech/Roche. E. Tsui is a consultant for EyePoint Pharmaceuticals (Watertown, MA), Kowa Company Ltd. (Nagoya, Japan), Cylite Pty Ltd. (Victoria, Australia). The other authors report no disclosures.

References

1. Dreyer RF, Gass DJ. Multifocal choroiditis and panuveitis. A syndrome that mimics ocular histoplasmosis. Arch Ophthalmol. 1984;102:1776–1784. [PubMed: 6508619]
2. Spaide RF, Goldberg N, Freund KB. Redefining multifocal choroiditis and panuveitis and punctate inner choroidopathy through multimodal imaging. Retina. 2013;33:1315–1324. [PubMed: 23584703]
3. Jampol LM, Wiredu A. MEWDS, MFC, PIC, AMN, AIBSE, and AZOOR: one disease or many? Retina. 1995;15:373–378. [PubMed: 8594628]
4. Jampol LM, Becker KG. White spot syndromes of the retina: a hypothesis based on the common genetic hypothesis of autoimmune/inflammatory disease. American Journal of Ophthalmology. 2003;135:376–379. [PubMed: 12614757]
5. Gass JD. Are acute zonal occult outer retinopathy and the white spot syndromes (AZOOR complex) specific autoimmune diseases? American Journal of Ophthalmology. 2003;135:380–381. [PubMed: 12614758]
6. Vance SK, Khan S, Klancnik JM, Freund KB. Characteristic spectral-domain optical coherence tomography findings of multifocal choroiditis. Retina. 2011;31:717–723. [PubMed: 21386760]
7. Essex RW, Wong J, Jampol LM, et al. Idiopathic multifocal choroiditis: a comment on present and past nomenclature. Retina. 2013;33:1–4. [PubMed: 23026849]
8. Spaide RF, Yannuzzi LA, Freund KB. Linear streaks in multifocal choroiditis and panuveitis. Retina. 1991;11:229–231. [PubMed: 1925089]
9. Fung AT, Pal S, Yannuzzi NA, et al. Multifocal choroiditis without panuveitis: clinical characteristics and progression. Retina. 2014;34:98–107. [PubMed: 23670288]
10. Standardization of Uveitis Nomenclature (SUN) Working Group. Classification Criteria for Multifocal Choroiditis With Panuveitis. Am J Ophthalmol. 2021;228:152–158. [PubMed: 33845016]
11. Abdelhakim AH, Yannuzzi LA, Freund KB, Jung JJ. DIFFERENTIAL RESPONSE TO GLUCOCORTICOID IMMUNOSUPPRESSION OF TWO DISTINCT INFLAMMATORY SIGNS ASSOCIATED WITH PUNCTATE INNER CHOROIDOPATHY. Retina. 2021;41:812–821. [PubMed: 32804829]
12. Orellana-Rios J, Leong BCS, Fernández-Avellaneda P, et al. LATE RECURRENCE OF CHOROIDAL NEOVASCULARIZATION IN PATIENTS WITH MULTIFOCAL CHOROIDITIS: CLINICAL SURVEILLANCE IN PERPETUITY. Retin Cases Brief Rep. 2022;16:233–241. [PubMed: 31725597]

13. Choudhry N, Duker JS, Freund KB, et al. Classification and Guidelines for Widefield Imaging: Recommendations from the International Widefield Imaging Study Group. Ophthalmol Retina. 2019;3:843–849. [PubMed: 31302104]
14. Essilfie J, Bacci T, Abdelhakim AH, et al. ARE THERE TWO FORMS OF MULTIPLE EVANESCENT WHITE DOT SYNDROME? Retina. 2022;42:227–235. [PubMed: 34432725]
15. Somkijrungroj T, Pearlman JA, Gonzales JA. Multifocal choroiditis and panuveitis presenting with progressive equatorial linear streaks: evolution of Schlaegel lines documented with multimodal imaging. Retin Cases Brief Rep. 2015;9:214–217. [PubMed: 25790317]
16. Scoles D, Bracha P, S Aleman T, et al. Diagnostic and Therapeutic Challenges. Retina. 2021;41:1999–2003. [PubMed: 33239546]
17. de Souza EC, de Campos VE, Duker JS. Atypical unilateral multifocal choroiditis in a COVID-19 positive patient. Am J Ophthalmol Case Rep. 2021;22:101034. [PubMed: 33623832]
18. Ramtohul P, Engelbert M, Malclès A, et al. BACILLARY LAYER DETACHMENT: MULTIMODAL IMAGING AND HISTOLOGIC EVIDENCE OF A NOVEL OPTICAL COHERENCE TOMOGRAPHY TERMINOLOGY: Literature Review and Proposed Theory. Retina. 2021;41:2193–2207. [PubMed: 34029276]
19. Flores-Moreno I, Lugo F, Duker JS, Ruiz-Moreno JM. The relationship between axial length and choroidal thickness in eyes with high myopia. Am J Ophthalmol. 2013;155:314–319.e1. [PubMed: 23036569]
20. Ramtohul P, Cabral D, Oh D, et al. En face Ultrawidefield OCT of the Vortex Vein System in Central Serous Chorioretinopathy. Ophthalmol Retina. 2022:S2468–6530(22)00487–0.
21. Jones BE, Jampol LM, Yannuzzi LA, et al. Relentless placoid chorioretinitis: A new entity or an unusual variant of serpiginous chorioretinitis? Arch Ophthalmol. 2000;118:931–938. [PubMed: 10900106]
22. Klufas MA, Phasukkijwatana N, Iafe NA, et al. Optical Coherence Tomography Angiography Reveals Choriocapillaris Flow Reduction in Placoid Chorioretinitis. Ophthalmol Retina. 2017;1:77–91. [PubMed: 31047399]
23. Marchese A, Agarwal AK, Erba S, et al. Placoid lesions of the retina: progress in multimodal imaging and clinical perspective. Br J Ophthalmol. 2022;106:14–25. [PubMed: 33468489]
24. Ramtohul P, Cabral D, Sadda S, et al. The OCT angular sign of Henle fiber layer (HFL) hyperreflectivity (ASHH) and the pathoanatomy of the HFL in macular disease. Prog Retin Eye Res. 2022:101135. [PubMed: 36333227]
25. Jung JJ, Khan S, Mrejen S, et al. Idiopathic multifocal choroiditis with outer retinal or chorioretinal atrophy. Retina. 2014;34:1439–1450. [PubMed: 24378424]
26. Moussa K, Alsberge JB, Munk MR, et al. IDIOPATHIC MULTIFOCAL CHOROIDITIS WITH SERPIGINOUS-LIKE PERIPAPILLARY CHORIORETINAL ATROPHY. Retina. 2022;42:1574–1582. [PubMed: 35333832]
27. Chen C, Cheng Y, Zhang Z, et al. CLINICAL CHARACTERISTICS OF STREAKY MULTIFOCAL CHOROIDITIS: A Subtype of Multifocal Choroiditis. Retina. 2022;42:2110–2119. [PubMed: 35839489]
28. Cicinelli MV, Marchese A, Ramtohul P, et al. PUNCTATE INNER CHOROIDOPATHY-LIKE REACTIONS IN UNRELATED RETINAL DISEASES. Retina. 2022;42:2099–2109. [PubMed: 36269801]
29. Ramtohul P, Cabral D, Cicinelli MV, Freund KB. RECURRENCE OF ACUTE RETINOPATHY IN PSEUDOXANTHOMA ELASTICUM. Retinal Cases and Brief Reports. 2022:10.1097/ICB.0000000000001363.
30. Cicinelli MV, Hassan OM, Gill MK, et al. A Multiple Evanescent White Dot Syndrome-like Reaction to Concurrent Retinal Insults. Ophthalmol Retina. 2021;5:1017–1026. [PubMed: 33348087]

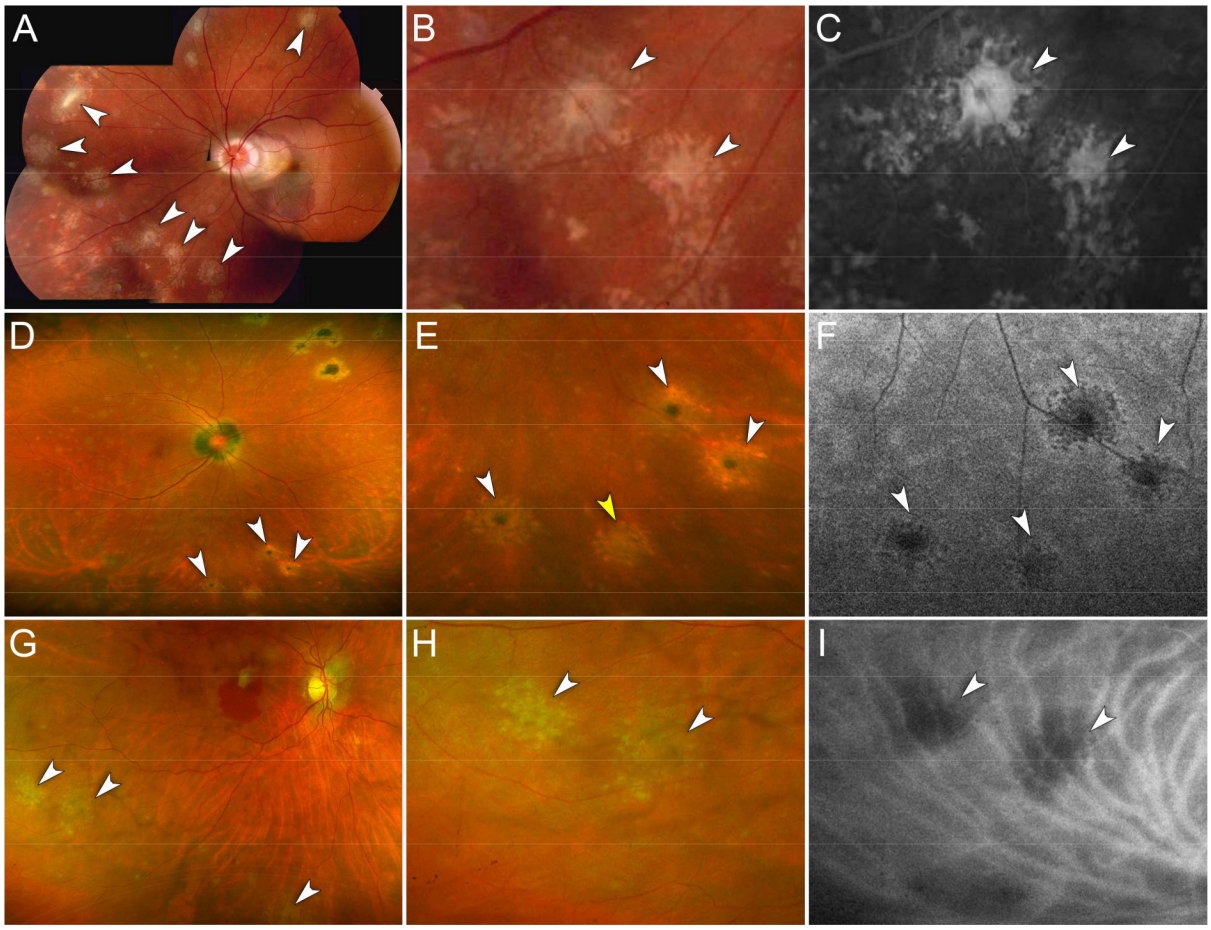

Figure 1. Representative cases of peripheral chrysanthemum lesions on multimodal imaging.

A – C. Case 1. Myopic female in her 30s.

A. Montage color fundus photography of the left eye shows multiple chrysanthemum lesions in the nasal and superior midperipheral retina (*white arrowheads*). Note the peripapillary subretinal hemorrhage associated with choroidal neovascularization in the macula.

B. Magnified view of (**A**). Chrysanthemum lesions are distinctively characterized by a grey-yellow central lesion surrounded by satellite dots (*white arrowheads*).

C. Magnified view of the fluorescein angiogram (late phase) showing hyperfluorescence of the chrysanthemum lesions (*white arrowheads*).

D – F. Case 11. Myopic female in her 40s.

D. Ultra-widefield pseudocolor fundus photography of the right eye shows multiple chrysanthemum lesions involving the inferior midperipheral retina (*white arrowheads*). Note the pre-existent punched-out chorioretinal scars in the supero-nasal retina and the peripapillary atrophy.

E. Magnified view of (**D**). Note the different degrees of pigmentation at the center of the chrysanthemum lesions suggesting the co-existence of recurrent lesions arising from pigmented scars (*white arrowheads*) and a new lesion with a grey-yellow center (*yellow arrowhead).*

F. Magnified view of fundus autofluorescence image showing hypoautofluorescent chrysanthemum lesions (*white arrowheads*).

G – I. Case 12. Myopic female in her 50s.

G. Ultra-widefield pseudocolor fundus photography of the right eye shows multiple chrysanthemum lesions in the inferior midperipheral retina (*white arrowheads*). Note mild vitritis and a subretinal hemorrhage in the macula associated with choroidal neovascularization.

H. Magnified view of (**G**). Chrysanthemum lesions are characterized by a grey-yellow central lesion surrounded by pale satellite dots (*white arrowheads*).

I. Magnified view of the indocyanine green angiogram (mid-phase) showing hypofluorescence of the chrysanthemum lesions (*white arrowheads*).

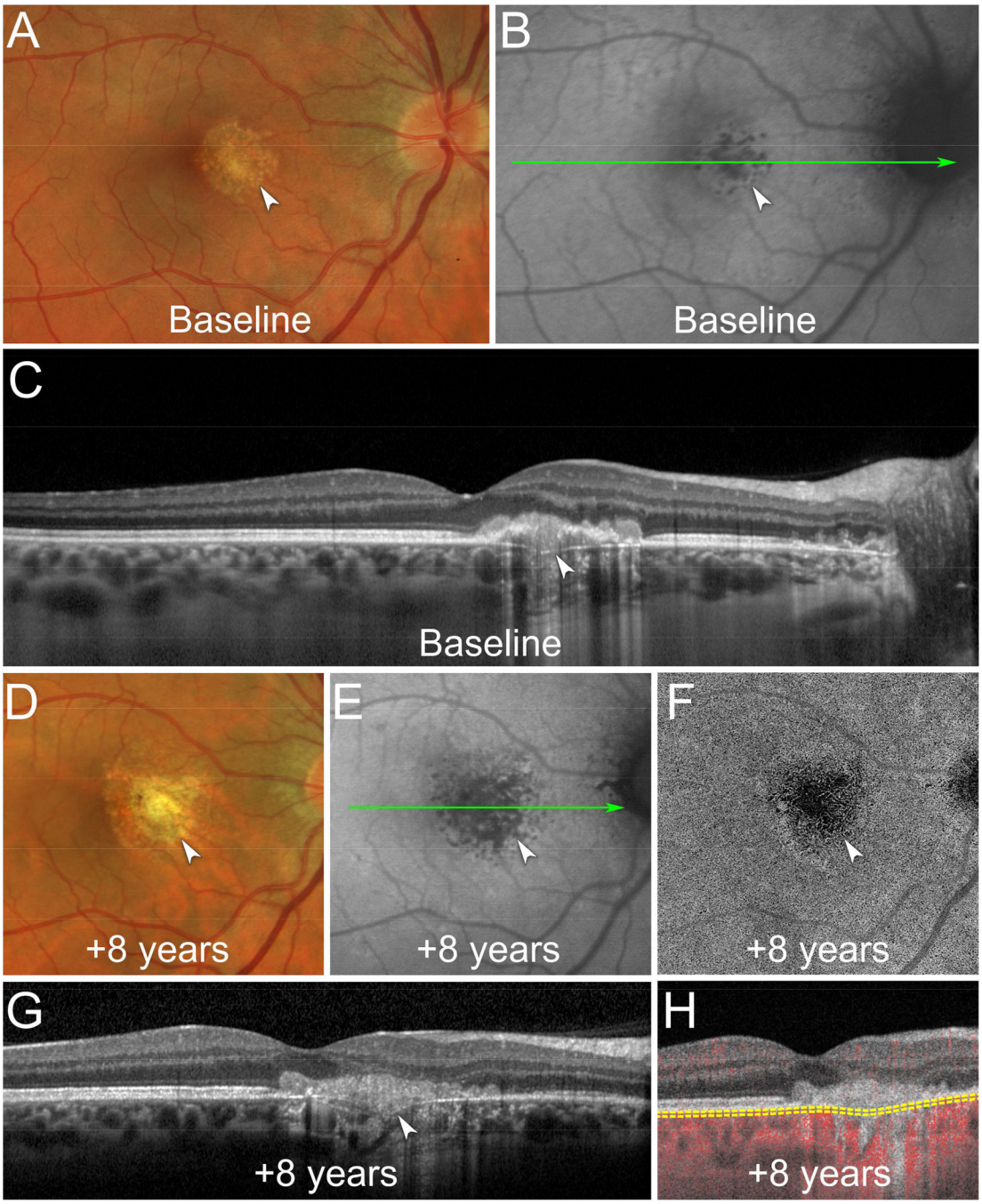

Figure 2. Multimodal imaging of a recurrent macular chrysanthemum lesion.

A. At baseline, color fundus photography shows a chrysanthemum lesion in the macula with a grey-yellow central lesion surrounded by pale satellite dots (*white arrowhead*).

B. Fundus autofluorescence image shows a hypoautofluorescent chrysanthemum lesion in the macula (*white arrowhead*). The green line indicates the location of the optical coherence tomography (OCT) B-scan displayed in (**C**).

C. OCT B-scan shows subretinal hyperreflective material splitting the retinal pigment epithelium/Bruch's membrane (RPE/BrM) complex, a downwardly deflected BrM defect,

and posterior choroidal hypertransmission (*white arrowhead*). The underlying choroid shows focal thickening and loss of the normal choroidal architecture.

D. At 8-year follow-up, color fundus photography shows recurrence of the chrysanthemum lesion (*white arrowhead*).

E. Fundus autofluorescence shows a larger hypoautofluorescent chrysanthemum lesion (*white arrowhead*). The green line indicates the location of the OCT B-scan displayed in (**G**).

F. En face swept-source OCT-angiography (OCTA) segmented at the level of the choriocapillaris shows flow signal deficit colocalizing with the chrysanthemum lesion (*white arrowhead*).

G. OCT B-scan shows a new hyperreflective material splitting the RPE/BrM complex (*white arrowhead*).

H. Cross-sectional OCTA shows flow signal deficits of the choriocapillaris colocalizing with the recurrent chrysanthemum lesion. The yellow dashed lines indicate the segmentation used to obtain the en face OCTA image displayed in (**F**).

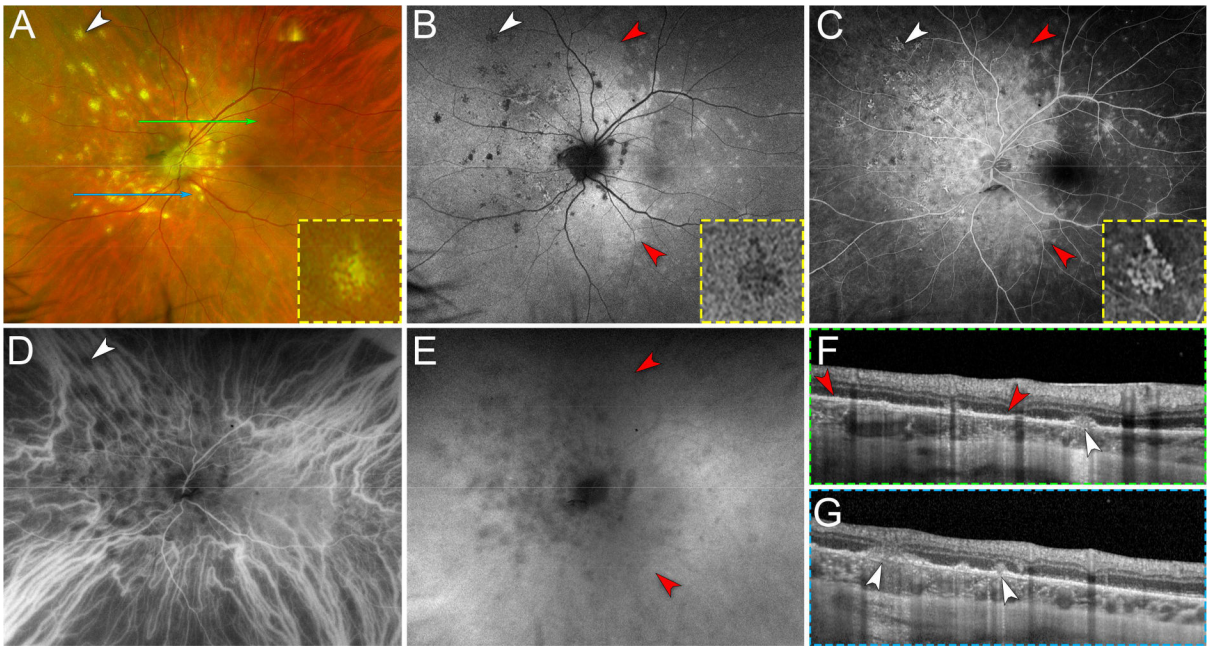

Figure 3. Multimodal imaging of chrysanthemum idiopathic multifocal choroiditis (iMFC) and epiphenomenon multiple evanescent white dot syndrome (EpiMEWDS).

A. Ultra-widefield pseudocolor fundus photography of the left eye shows multiple chrysanthemum lesions in the posterior pole and nasal midperipheral retina (*white arrowhead*). The inset (*yellow dashed box*) is a magnified view of the chrysanthemum lesion annotated with the *white arrowhead*. Note the distinctive morphology of the chrysanthemum lesion characterized by a grey-yellow central lesion surrounded by satellite dots. The green and blue lines indicate the location of the optical coherence tomography (OCT) B-scans displayed in (**F**) and (**G**), respectively.

B. Ultra-widefield fundus autofluorescence image shows hypoautofluorescent chrysanthemum lesions (*white arrowhead*). The inset (*yellow dashed box*) is a magnified view of the hypoautofluorescent chrysanthemum lesion annotated with the *white arrowhead.* Note the areas of hyperautofluorescence surrounding the chrysanthemum lesions and the scattered hyperautofluorescent spots corresponding to EpiMEWDS (*red arrowheads*).

C. Late phase of ultra-widefield fluorescein angiogram shows hyperfluorescent chrysanthemum lesions (*white arrowhead*) surrounded by confluent hyperfluorescent areas corresponding to EpiMEWDS (*red arrowheads*). The inset (*yellow dashed box*) is a magnified view of the hyperfluorescent chrysanthemum lesion annotated with the *white arrowhead.*

D. Early phase of ultra-widefield indocyanine green angiogram shows hypofluorescent chrysanthemum lesion distributed along and at the tips of the nasal vortex veins (*white arrowhead*).

E. Late phase of ultra-widefield indocyanine green angiogram shows confluent hypofluorescent areas corresponding to EpiMEWDS (*red arrowheads*).

F and **G**. Spectral-domain OCT B-scans show chrysanthemum lesions characterized by subretinal hyperreflective material (*white arrowheads*) splitting the retinal pigment epithelium/Bruch's membrane, posterior hypertransmission, focal choroidal thickening and

loss of the normal choroidal architecture. Note the areas of ellipsoid and interdigitation zone disruption (between *red arrowheads* in **F**) corresponding to EpiMEWDS.

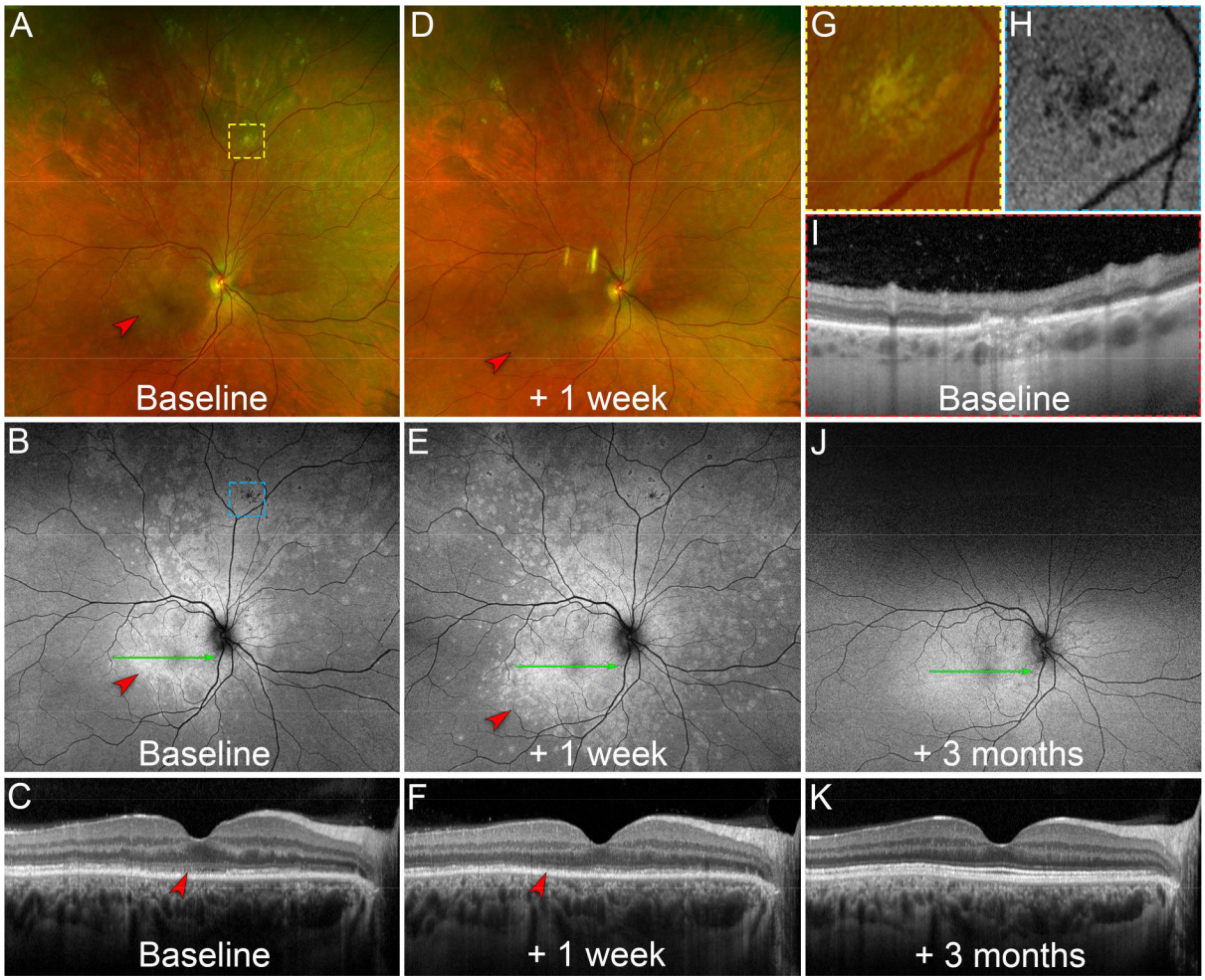

Figure 4. Differential responses of chrysanthemum idiopathic multifocal choroiditis (iMFC) and epiphenomenon multiple evanescent white dot syndrome (EpiMEWDS) to corticosteroid therapy.

A. At baseline, ultra-widefield pseudocolor fundus photography of the right eye shows chrysanthemum lesions in the superior mid- and far-peripheral retina (*yellow dashed box*). Note the multifocal white lesions in the macula (*red arrowhead*) corresponding to EpiMEWDS. The yellow dashed box indicates the location of the magnified view displayed in (**G**).

B. Baseline ultra-widefield fundus autofluorescence image shows hypoautofluorescent chrysanthemum lesions superiorly (*blue dashed box*) and hyperautofluorescent areas corresponding to EpiMEWDS (*red arrowhead*). The blue dashed box indicates the location of the magnified view displayed in (**H**). The green line indicates the location of the optical coherence tomography (OCT) B-scan displayed in (**C**).

C. Baseline OCT B-scan shows disruption of the ellipsoid (EZ) and interdigitation zones (IZ) in the macula corresponding to EpiMEWDS (*red arrowhead*). The patient's visual acuity was 20/80 in the right eye.

D. After 1 week of oral corticosteroid (1mg/kg/day), ultra-widefield pseudocolor fundus photography shows regression of the chrysanthemum lesions superiorly without new lesions.

Note the paradoxical extension of the multifocal white lesions in the macula (*red arrowhead*) corresponding to EpiMEWDS.

E. At 1-week, ultra-widefield fundus autofluorescence image shows stable hypoautofluorescent chrysanthemum lesions. Note the extension of the hyperautofluorescent EpiMEWDS in the macula (*red arrowhead*). The green line indicates the location of the OCT B-scan displayed in (**F**).

F. At 1-week, OCT B-scan shows extension of the EZ and IZ disruption in the macula (*red arrowhead*). The patient's visual acuity decreased to 20/200 in the right eye.

G. Magnified view of the chrysanthemum lesion at baseline on pseudocolor fundus photography. Note the distinctive morphology of the chrysanthemum lesion characterized by a grey-yellow central lesion surrounded by satellite dots.

H. Magnified view of the hypoautofluorescent chrysanthemum lesion at baseline on fundus autofluorescence imaging.

I. Baseline OCT B-scan through the chrysanthemum lesion displayed in (**G**) and (**H**). Note the subretinal hyperreflective material splitting the retinal pigment epithelium/Bruch's membrane and associated with posterior hypertransmission, focal choroidal thickening and loss of the normal choroidal architecture.

J. After 3 months and gradual taper of the corticosteroid therapy, ultra-widefield fundus autofluorescence image shows regression of the hyperautofluorescent EpiMEWDS. The green line indicates the location of the OCT B-scan displayed in (**K**).

K. At 3-month, the OCT B-scan shows restoration of the EZ/IZ bands in the macula. The patient's visual acuity improved to 20/20 in the right eye.

Table 1.

Demographic and clinical data of patients with idiopathic multifocal choroiditis and chrysanthemum lesions.

Characteristics	***Number***
No. of patients	20
No. of eyes	25
Age (mean years ± SD)	35.8 ± 17.0
Follow-up duration (mean months, range)	15 (3 – 96)
Gender n (%)	
Male	8/20 (4.0%)
Female	12/20 (60.0%)
Refractive error n (%)	
Myopic	24/25 (96.0%)
Emmetropic	1/25 (4.0%)
SE (mean diopters, range)	−5.50 (−12.0 to 0)
BCVA (mean Snellen equivalent)	
Initial	20/33
Final	20/26
Presenting symptom, n (%)	
Vision loss	15/20 (75.0%)
Scotoma	5/20 (25.0%)
Photopsia	1/20 (5.0%)
Treatments n (%)	
Oral corticosteroid	18/20 (90.0%)
Periocular corticosteroid	2/20 (10.0%)
Immunosuppressive therapy	2/20 (10.0%)

Abbreviations: BCVA: best-corrected visual acuity; SE: spherical equivalent

Table 2.

Multimodal imaging characteristics of patients with idiopathic multifocal choroiditis and chrysanthemum lesions.

Multimodal Imaging Modality	***Features***
Clinical examination	Grey-yellow central lesion surrounded by pale satellite dots Location: posterior pole (48.0%) / mid- and far-periphery exclusively (52.0%) Number of lesions: 1 (16.0%) > 2 and < 19 (28.0%) > 20 and < 49 (40.0%) < 50 (16.0%) Associated findings: none (52.0%) punched-out chorioretinal scars (40.0%) Schlaegel lines (4.0%) peripapillary atrophy (4.0%) Anterior segment inflammation and vitritis (16.0%)
Optical coherence tomography	Subretinal iso/hyperreflective material splitting the RPE/BrM complex Downwardly deflected defect of BrM Posterior choroidal hypertransmission Focal choroidal thickening Hyporeflectivity and loss of the normal choroidal architecture
Optical coherence tomography angiography	Flow signal deficit of the choriocapillaris and inner choroid
Fundus autofluorescence	Hypoautofluorescence
Fluorescein angiography	Early and late hyperfluorescence
Indocyanine green angiography	Early and late hypofluorescence

Abbreviations: RPE/BrM: retinal pigment epithelium/Bruch’s membrane